Synthesis and decay properties of isotopes of element 110: ^{273}Ds and ^{275}Ds

Yu. Ts. Oganessian,[1] V. K. Utyonkov,[1] M. V. Shumeiko,[1] F. Sh. Abdullin,[1] G. G. Adamian,[1] S. N. Dmitriev,[1] D. Ibadullayev,[1,2] M. G. Itkis,[1] N. D. Kovrizhnykh,[1] D. A. Kuznetsov,[1] O. V. Petrushkin,[1] A. V. Podshibiakin,[1] A. N. Polyakov,[1] A. G. Popeko,[1] I. S. Rogov,[1] R. N. Sagaidak,[1] L. Schlattauer,[1,3] V. D. Shubin,[1] D. I. Solovyev,[1] Yu. S. Tsyganov,[1] A. A. Voinov,[1] V. G. Subbotin,[1] N. S. Bublikova,[1] M. G. Voronyuk,[1] A. V. Sabelnikov,[1] A. Yu. Bodrov,[1] N. V. Aksenov,[1] A. V. Khalkin,[1] Z. G. Gan,[4] Z. Y. Zhang,[4] M. H. Huang,[4] and H. B. Yang[1,4]

[1]*Joint Institute for Nuclear Research, RU-141980 Dubna, Russian Federation*
[2]*L.N. Gumilyov Eurasian National University, 010000 Astana, Kazakhstan*
[3]*Palacky University Olomouc, Department of Experimental Physics, Faculty of Science, 771 46 Olomouc, Czech Republic*
[4]*Institute of Modern Physics, Chinese Academy of Sciences, Lanzhou 730000, China*

(Received 29 February 2024; accepted 19 April 2024; published 6 May 2024)

The ^{232}Th(^{48}Ca, $5n$)^{275}Ds and ^{238}U(^{40}Ar, $5n$)^{273}Ds reactions have been studied at the gas-filled separator DGFRS-2 at the Superheavy Element Factory at Flerov Laboratory of Nuclear Reactions, Joint Institute for Nuclear Research. For the first time, a new isotope ^{275}Ds with a half-life of $0.43^{+0.29}_{-0.12}$ ms and α-particle energy of 11.20 ± 0.02 MeV was synthesized in the ^{48}Ca-induced reaction with the actinide nucleus and identified by measuring correlated α decays ending in known nuclei. The decay properties of nuclei originating from ^{273}Ds and ^{275}Ds are compared with theoretical calculations and decay schemes are proposed. The cross sections of the ^{232}Th(^{48}Ca, $5n$)^{275}Ds reaction of $0.11^{+0.46}_{-0.09}$ and $0.34^{+0.59}_{-0.16}$ pb were measured at excitation energies of the ^{280}Ds compound nucleus $E^* = 51$ and 56 MeV, respectively. The cross section of the $5n$-evaporation channel of the ^{238}U + ^{40}Ar reaction at $E^* = 49$ MeV of $0.18^{+0.44}_{-0.12}$ pb turned out to be comparable to that for ^{275}Ds at close excitation energy.

DOI: 10.1103/PhysRevC.109.054307

I. INTRODUCTION

It is known that the existence of transactinide elements ($Z \geqslant 104$) is directly determined by the structure of their nuclei. The decay properties of more than 100 isotopes obtained over 50 years in experiments on the synthesis of elements with $Z = 106-118$ have generally confirmed the predictions of the shell model of the nucleus about the existence of regions (islands) of stability. This circumstance has greatly changed previously existing ideas about the limits of the masses of nuclei. Now, according to the decay properties of superheavy nuclides, it has been established that the boundary of the masses of the nuclei shifts to the region $A \geqslant 300$. In theory, the phenomenon of the amazing survivability of the heaviest nuclides is explained by the appearance and action of new closed nuclear shells of protons $Z = 108$ and neutrons $N = 162$ (deformed nuclei), and heavier (superheavy) nuclei with $Z = 114-126$, $N = 184$, which in the ground state have a spherical shape, like the doubly magic ^{208}Pb.

Of particular interest are also the nuclei located between the above shells, where the effect of the shells is minimal, the nuclei in the ground state change shape, the height of the fission barrier is almost halved, and their stability decreases significantly, both with respect to α decay and spontaneous fission (SF). This is the region of nuclei in the vicinity of $Z = 110-111$ and $N = 168-170$.

Studies of such nuclei have been extremely limited until recently due to the very small cross section of their formation. Now, after receiving intense beams at the new DC280 accelerator and commissioning the new DGFRS-2 recoil separator at the Superheavy Element Factory (SHE Factory) at Flerov Laboratory of Nuclear Reactions (FLNR), Joint Institute for Nuclear Research (JINR), we return to this task again. In the recently completed first experiment, in the fusion reaction ^{232}Th + ^{48}Ca, a new isotope of element 110 with a mass of 276 was synthesized for the first time in the $4n$-evaporation channel [1]. For the new isotope ^{276}Ds, the decay properties and the cross section of its formation ($\sigma \approx 0.7$ pb) were determined. The α decay products of ^{276}Ds were also previously unknown isotopes of elements 108 and 106: ^{272}Hs ($N = 164$) and ^{268}Sg ($N = 162$). The energies and probabilities of α decay and spontaneous fission were also determined for them. Note that all members of the radioactive family ^{276}Ds(α, SF) $\rightarrow$ ^{272}Hs(α) $\rightarrow$ ^{268}Sg(SF) are located in proximity to the doubly magic ^{270}Hs with closed deformed shells $Z = 108$, $N = 162$. The new nuclides, according to the theory, also belong to the family of nuclei with large deformations.

The present paper is a continuation of these studies. In the ^{232}Th + ^{48}Ca reaction, the excitation energy of the ^{280}Ds compound nucleus was increased, which made it possible for the first time to synthesize odd isotope ^{275}Ds ($N = 165$) in the $5n$-evaporation channel and determine its decay properties. Another lighter isotope, ^{273}Ds ($N = 163$), was also produced in the $5n$-evaporation channel of the ^{238}U + ^{40}Ar fusion reaction.

The experiment is described below, and experimental data are presented.

TABLE I. The ^{232}Th and ^{238}U target thicknesses; reaction-specific laboratory-frame projectile energies E_{lab} in the middle of the target layers; resulting excitation energy E^* intervals (with use of mass tables [4,5]); total beam doses; the numbers of observed decay chains of ^{276}Ds (4n), ^{275}Ds (5n), and ^{273}Ds (5n); and the cross sections σ of their production.

Reaction	Target thickness (mg/cm^2)	E_{lab} [a] (MeV)	E^* (MeV)	Beam dose $\times 10^{19}$	No. of chains $4n/5n$	σ_{4n} (pb)	σ_{5n} (pb)
^{232}Th + ^{48}Ca	0.65	250.6	48.9–52.3	2.0	1/1	$0.11^{+0.46}_{-0.09}$ [b]	$0.11^{+0.46}_{-0.09}$
		257.0	54.2–57.5	3.2	0/5	<0.2	$0.34^{+0.59}_{-0.16}$
^{238}U + ^{40}Ar	0.69	212.2	47.5–50.7	3.2	0/2	<0.3	$0.18^{+0.44}_{-0.12}$

[a]The beam energy was measured with a systematic uncertainty of 1 MeV.
[b]The result for the 4n-evaporation channel taken from Ref. [1].

II. EXPERIMENT

The experiments were performed at the gas-filled separator DGFRS-2 [2] online to the new cyclotron DC280 at the SHE Factory at FLNR, JINR [3]. Some parameters of the experiments, as well as a number of the observed nuclei and cross sections of their production in the ^{232}Th + ^{48}Ca and ^{238}U + ^{40}Ar reactions, are listed in Table I.

Twelve target sectors were produced by electrodeposition on 0.62-mg/cm^2 Ti backing and were mounted on a disk with a diameter of 24 cm, which was rotated at 980 rpm, similar to Refs. [1,6]. The α activity of the targets used is quite small. For periodical monitoring of the stability of the target during the experiment, we added about 15–20 μg of ^{243}Am to the target, which allowed us to register 5.3-MeV α particles by the focal detector after changing the setting of the DGFRS-2 magnets for their maximum transmission. The beam intensity at the target was reduced to 3 p μA, compared with Refs. [1,6].

The nuclei recoiling out from the target pass through hydrogen at a pressure of 0.9 mbar inside DGFRS-2, 0.7-μm Mylar separating foil, two multiwire proportional chambers located in pentane at a pressure of 1.6 mbar, and are implanted into detectors. The separator magnetic rigidities were set to 2.43 and 2.56 T m in experiments with ^{232}Th and ^{238}U, respectively.

The focal detector consisted of two 48 × 128-mm^2 double-sided strip detectors [BB17 (DS)-300] with 48 1-mm horizontal strips on the front side and 128 1-mm-wide vertical strips on the back one. The first detector shielded a part of the rear detector. The back strips were paired together to form 110 strips of 2-mm width. This detector was surrounded by eight 60 × 120-mm^2 side detectors (W4-300), each with eight strips, constituting a box with a depth of 120 mm. The signals in the focal and side detectors with amplitudes above thresholds of ≈0.2 and ≈2.7 MeV, respectively, were recorded independently by digital and analog data acquisition systems (see Refs. [1,2,6–9] for details).

III. RESULTS AND DISCUSSION

The energies of α particles or spontaneous fission fragments and decay times of nuclei in the decay chains of ^{275}Ds observed in the ^{232}Th + ^{48}Ca experiments are shown in Fig. 1.

The decay properties of daughter and descendant nuclei of ^{275}Ds are in good agreement with those observed in the five α-SF chains and one α-α-SF chain in the ^{248}Cm + ^{26}Mg reaction and assigned to the parent nucleus ^{271}Hs [10], namely, ^{271}Hs ($T_{1/2} \approx 4$ s, $E_\alpha = 9.13 \pm 0.05$ and 9.30 ± 0.05 MeV), ^{267}Sg ($E_\alpha = 8.20 \pm 0.05$ MeV, $b_{a/\mathrm{SF}} = 0.17/0.83$, $T_{1/2} = 80^{+60}_{-20}$ s), and ^{263}Rf ($T_{\mathrm{SF}} = 8^{+40}_{-4}$ s). Thus, for the first time, a new superheavy nucleus was produced in the reaction of ^{48}Ca with an isotope of an actinide element, ^{232}Th, and was identified by the method of genetic relations [11]. This was done by establishing a unique relationship between the radioactive decays of ^{275}Ds and the known properties of its descendants ^{271}Hs, ^{267}Sg, and ^{263}Rf.

At the same time, our new results can be considered a confirmation of the results [10] that were obtained by one group with the use of the same apparatus. In addition, the data from Ref. [10] previously contradicted results, where SF activity with $T_{\mathrm{SF}} = 10 - 24$ min was observed after a specific group-4 chemical separation and was attributed to ^{263}Rf, the product of a ≈3% electron capture branch for ^{263}Db (see Ref. [12] and references therein). Thus, the results of Ref. [10] and this paper did not confirm the assumption of the existence of such a decay mode for ^{263}Db.

In the experiments [10], a rapid chemical isolation of Hs isotopes was used, which does not allow measuring the decay times of the mother nucleus. On the other hand, the measured lifetimes of the daughter nucleus ^{267}Sg varied in the range from 30 to 264 s, but the interval for registration of α-α and α-SF sequences did not exceed 300 s. As can be seen in Fig. 1, four of the six chains could not be registered in the ^{248}Cm + ^{26}Mg experiment [10]. Under these experimental conditions, the method of determining the half-life proposed in Ref. [13] could not be used. Another method [14], which provides an opportunity to obtain estimates of the half-life with a limited measurement interval, does not allow one to determine the upper limit of the half-life for the observed set of decay times. For the calculation of the half-life of ^{267}Sg, we used method [14], and the results of this paper have been added by the data from Ref. [10] with a measurement interval of 300 s.

In the decay chains observed in Ref. [10] for ^{271}Hs, one can notice a feature: five chains that began with α decay with $E_\alpha = 9.1$ MeV ended with SF with decay times $\tau = 30$–264 s, and in one chain with $E_\alpha = 9.3$ MeV of the first decay an additional α decay with $E_\alpha = 8.2$ MeV and $\tau = 149$ s was detected, which was followed by SF after 12 s. A similar decay pattern was observed in the chains shown in Fig. 1: in three chains with $E_\alpha = 9.05$ MeV of ^{271}Hs, subsequent

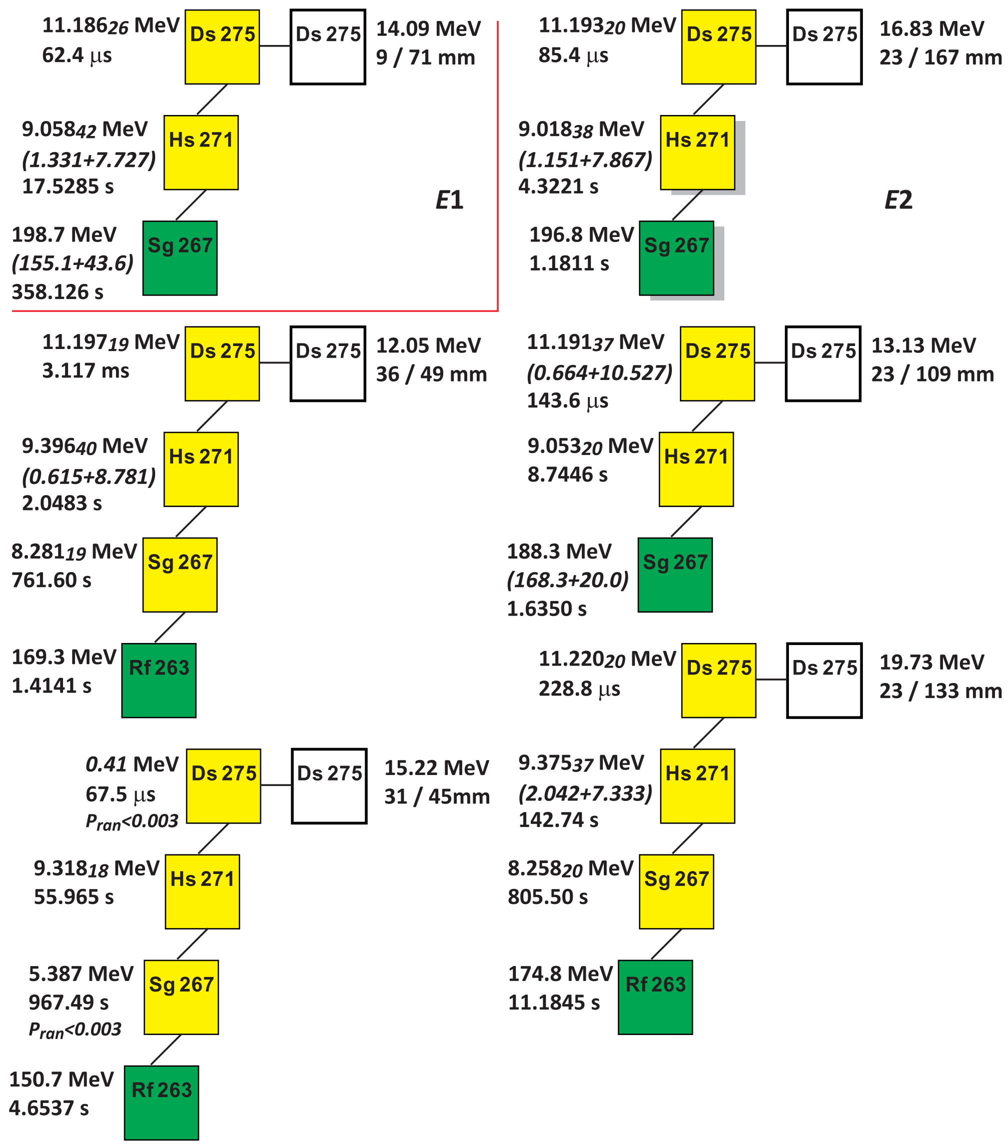

FIG. 1. Decay chains originating from ^{275}Ds observed in the ^{232}Th + ^{48}Ca reaction at the projectile energies $E1 = 250.6$ MeV and $E2 = 257.0$ MeV. The rows on the right side show evaporation residue (ER, blank square) energies and vertical and horizontal positions on the detector (in mm). The left rows provide the α particle [in yellow (light gray)] and SF [in green (dark gray)] energies and time intervals between the events. The energies of the summed signals are given in parentheses. The events marked with a shadow were registered during the beam-off periods (see Refs. [1,2,6–9] for details). The α-particle energy errors are shown by smaller italic numbers. The probabilities of random origin of two events $P_{\rm ran}$ are shown; these particles escaped the focal detector, leaving low energy in it, but did not enter the side detector.

SF was recorded with $\tau = 1$–358 s, and in the other three chains of ^{271}Hs with $E_\alpha = 9.34$ MeV subsequent α decays with $E_\alpha = 8.27$ MeV and $\tau = 762$–967 s were also registered, which were then terminated by SF with $\tau = 1$–11 s.

The measured α-particle energies of the mother nucleus ^{275}Ds are similar, and the decay times do not indicate possible decays with different half-lives. In particular, the standard deviation of the logarithm of the measured decay times $[\sigma(\ln t)_{\rm exp} = 1.35]$ of ^{275}Ds satisfies the criterion proposed in Ref. [15] for a single exponent ($\sigma_{\rm lim} = 0.48-1.89$). However, some difference in the α-particle energy of ^{271}Hs and in the decay mode of the subsequent isotope ^{267}Sg, observed in two different experiments, suggests the presence of decays through different excited levels.

Therefore, we evaluated the properties of isotopes ^{271}Hs and ^{267}Sg separately for different decay branches. It turned out that not only do these isotopes decay with different α-particle energies (^{271}Hs) or decay modes (^{267}Sg), but their half-lives also differ markedly. Moreover, the errors in determining the half-lives do not overlap for a confidence level of 68%. The experimental decay properties of nuclei in the ^{275}Ds chain are given in the first five columns of Table II.

We also estimated the hindrance factors for α-decaying nuclei as $\mathrm{HF} = T^{\rm exp}/T^{\rm calc}$, where experimental half-lives were

TABLE II. Summary of decay properties of nuclei synthesized in the $^{232}Th + ^{48}Ca$ reaction in the present paper. The first three columns show the nucleus, decay mode, and experimental half-life. The next five columns show α-particle energy E_α, α-decay energy Q_α, as well as calculated spin and partial half-lives with respect to α decay and SF.

Nucleus	Decay mode	$T^{\rm exp}_{1/2}$	E_α (MeV)[a]	Q_α (MeV)[a]	Spin	$T^{\rm calc}_{a}$	$T^{\rm calc}_{\rm SF}$
^{275}Ds	α	$0.43^{+0.29}_{-0.12}$ ms	11.20(2)	11.37(2)	3/2	0.22 ms	2.0 s
^{271}Hs	α	$7.1^{+8.4}_{-2.5}$ s	9.05(2)	9.18(2)	3/2	5.1 s	6.0 min
^{271}Hs	α	46^{+56}_{-16} s	9.34(2)	9.48(2)	11/2	63 s	21 h
^{267}Sg	SF	100^{+92}_{-39} s[b]			1/2	16 h	140 s
^{267}Sg	α	$9.8^{+11.3}_{-4.5}$ min[b]	8.27(2)	8.40(2)	9/2	6 min	2.9 h
^{263}Rf	SF	$5.1^{+4.6}_{-1.7}$ s[b]			1/2	0.5 h	6.4 s

[a]Energy uncertainties (standard deviations) given in parentheses correspond to the data with the best energy resolution.
[b]Half-lives are calculated from the results of Ref. [10] and the present paper.

taken from Ref. [10] and this paper and calculated ones from several formulas for even-even nuclei. Among the many formulas available in the literature, we used the Viola-Seaborg formula with the parameters fitted in Ref. [16], as well as the formula in Ref. [17], which was used in spectroscopy studies of superheavy nuclei (see Ref. [18] and later works, e.g., Ref. [19]). In addition, we used three more recently proposed formulas [20–22], which were chosen taking into account the standard deviation of $\log_{10}[T^{\rm exp}/T^{\rm calc}]$ values for 12 known even-even nuclei with $Z = 106-114$, including ^{276}Ds and ^{272}Hs [1]. These standard deviations range from 0.16–0.17 [17,20,21] to 0.21 [16] and 0.24 [22]. For the same isotopes, the average differences of $\log_{10}[T^{\rm exp}/T^{\rm calc}]$ were determined, and these shifts, which varied from $-0.04-0.14$ [16,21,22] to 0.35 [17] and 0.48 [20], were then taken into account when calculating $T^{\rm calc}$. These hindrance factors are shown in Fig. 2 separately as intervals determined by formulas in Refs. [16,17,20,21] and a value obtained by the formula in Ref. [22], since in all cases the latter value falls out of the intervals, possibly due to the maximum standard deviation of all.

Using the experimental Q_α values, α-decay and spontaneous fission half-lives $T^{\rm exp}_{{\rm SF},\alpha}$, and the fission model of Refs. [23,24], we extract the decay schemes (the spins and energies of the one-quasiparticle states) for isotopes stemming from the α-decay chain of ^{275}Ds (see Fig. 2 and Table II). An advantage of the employed fission model is the simultaneous description of the α decay and SF from ground and isomeric states of both even-even and even-odd nuclei with the same set of parameters. The main assumption of this model is that charge asymmetry, as the corresponding collective variable, is responsible for these processes. The SF and α-cluster states are fully described by the stationary Schrödinger equation in the charge asymmetry coordinates. The calculated absolute values of SF and α-decay half-lives of even-even and even-odd nuclei in the ground state are in good agreement with the existing experimental data [1,7,23]. As shown for the fissioning even-odd nuclei [24], the centrifugal potential strongly affects the shape of the driving potential in the region of asymmetric dinuclear systems (especially the system with α particles as the light cluster), increasing the potential energy, for example, the height of the potential barrier, and finally creating the fission hindrance. So, the origin of the SF hindrance is related to the spin dependence of the formation probabilities of the asymmetric and symmetric binary cluster configurations, which are attributed to SF, and the hindrance factor is the degree of spin-hindered fission. This fact allows us to predict the spin of a quasiparticle state, knowing its experimental half-life and Q_α value.

The extracted one-quasiparticle spectra and the most probable α decays and SF are presented in Fig. 2 for the nuclei of the α decay chain containing ^{275}Ds (Table II). Odd-A nuclei mainly decay by emitting an α particle to the states with a similar spin and parity in the daughter nuclei. The ground state of ^{275}Ds decays to the long-lived isomeric state 3/2 in ^{271}Hs.

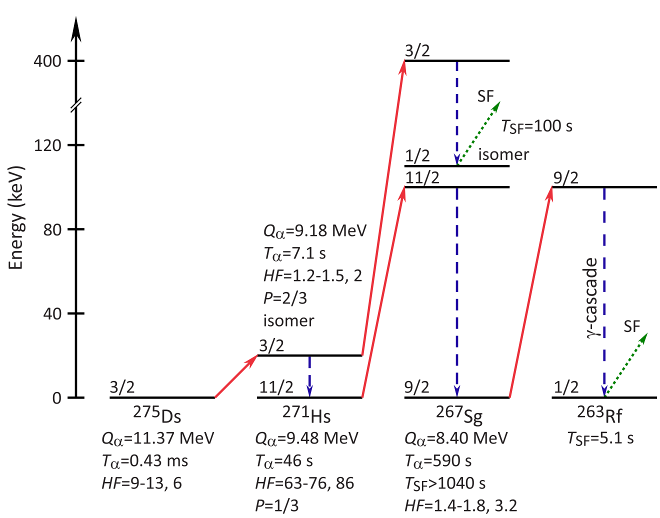

FIG. 2. A proposed experimental and calculated decay scheme for ^{275}Ds based on present and previously published data [10]. Alpha or γ transitions to approximate one-quasiparticle states and SF decays are shown by red (solid), blue (dashed), and green (dotted) lines, respectively. Alpha-decay energies (Q_α) and half-lives are provided for states decaying by α decay (T_α) or spontaneous fission ($T_{\rm SF}$). Hindrance factors $HF = T^{\rm exp}_{1/2} / T^{\rm calc}_{1/2}$ were derived from experimental and calculated half-lives according to Refs. [16,17,20–22] (see text). Population probabilities P of energy levels for ^{271}Hs are based on experimental data [10] and this paper.

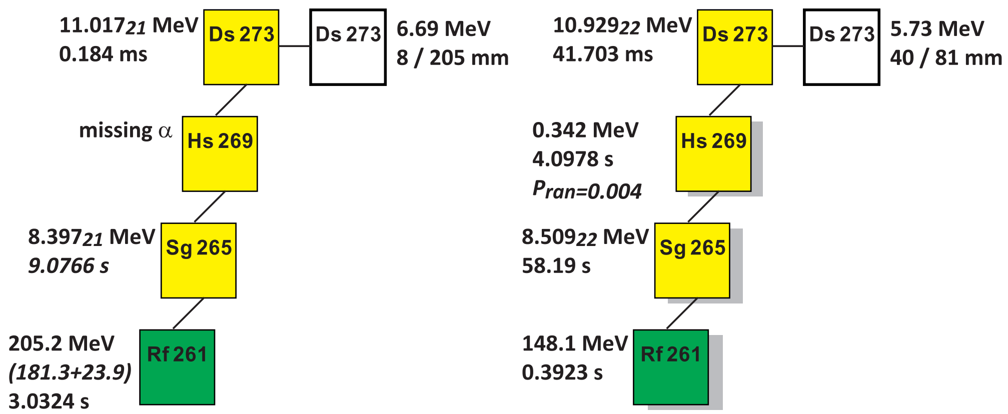

FIG. 3. The same as in Fig. 1, but for ^{273}Ds observed in the ^{238}U + ^{40}Ar reaction at the projectile energy of 212.2 MeV. The time interval for an α particle with $E_\alpha = 8.397$ MeV following a "missing α" was measured from a preceding α decay with $E_\alpha = 11.017$ MeV and is shown in italic.

The ground state 11/2 of ^{271}Hs is partly populated by the deexcitation of this higher-lying isomer. The α decay of ^{271}Hs occurs from both the ground state (11/2) and the isomeric state (3/2). The further decay channels are the following:

$$^{271}\text{Hs}(3/2) \rightarrow {}^{267}\text{Sg}(3/2) \rightarrow {}^{267}\text{Sg}(1/2) \rightarrow \text{SF}$$

and

$$^{271}\text{Hs}(11/2) \rightarrow {}^{267}\text{Sg}(11/2) \rightarrow {}^{267}\text{Sg}(9/2) \rightarrow {}^{263}\text{Rf}(9/2) \rightarrow {}^{263}\text{Rf}(1/2) \rightarrow \text{SF}.$$

In the first case, the excited state 3/2 of ^{267}Sg is populated, from which γ decay to lower-lying low-spin isomeric state 1/2 leads to the SF of ^{267}Sg. As seen in Fig. 2, the α decay from the ground state 11/2 of ^{271}Hs only populates the states with large spin (9/2, 11/2) in ^{267}Sg and ^{263}Rf. However, in ^{263}Rf, the cascade of γ transitions from higher state 9/2 populates low-spin ground or isomeric states, leading to the SF. Thus, the SF in ^{267}Sg and ^{263}Rf is related to the lowest-spin (1/2) isomeric or ground states. As is clear, the SF from low-spin states occurs faster than from high-spin states in an odd-A nucleus. Note that the presence of isomeric states 1/2 and 3/2, respectively, in ^{267}Sg and ^{271}Hs is predicted in Ref. [25].

In the ^{238}U + ^{40}Ar reaction at an excitation energy of 49 MeV, the 5n-evaporation channel is the most likely. The isotope ^{273}Ds was previously identified in five decay chains of ^{277}Cn [26,27]. Note that the properties of the nuclei in the decay chains of isotopes ^{272,274,275}Ds —products of the 6n, 4n, and 3n channels, respectively—differ from the properties of the nuclei in the chains shown in Fig. 3. Namely, the α-particle energies of the nuclei in the ^{273}Ds chains differ from the properties of the nuclei in the ^{275}Ds decay chains, a product of the 3n channel of this reaction (compare with the data in Fig. 1 and Table II).

The properties of even-even nuclei in the decay chains of ^{272,274}Ds —products of the 4n- and 6n-reaction channels, the decay of which through ground states with certain energies is more likely—also differ from those shown in Fig. 3. For example, from empirical systematics of α-decay energies vs neutron number, one can expect the energy of α particles of about 11.4 and 10.5 MeV for ^{274}Ds and ^{272}Ds, respectively (see, e.g., Fig. 2 in Ref. [1]). The E_α values for ^{270}Hs and ^{268}Hs are known, viz., 9.02 [28], 8.88 [10], or 9.02 MeV [29] for ^{270}Hs and 9.48 MeV [30] for ^{268}Hs. For the final spontaneously fissioning nuclei of ^{266}Sg and ^{264}Sg, the half-lives are 300 ms [10,28,29] and 68 ms [31], respectively.

Therefore, we assign the observed chains to the isotope ^{273}Ds (see Fig. 3). The existence of two states in the isotopes ^{265}Sg and ^{261}Rf (hereinafter referred to as ^{265}Sg^a, ^{265}Sg^b, ^{261}Rf^a, and ^{261}Rf^b) was proposed in Ref. [32]. Spontaneous fission was observed only in one of the two decay branches of the isotope ^{261}Rf^b with $T_{\text{SF}} = 2.6^{+0.7}_{-0.5}$ s [33], and no SF was recorded for ^{257}No (SF branch <0.015 [31]). Thus, the last nucleus in the chains should be attributed to the isotope ^{261}Rf^b.

The measured α-particle energy and the decay time for ^{273}Ds in the first (left) decay chain shown in Fig. 3 are in agreement with the values observed in Refs. [26,27] [E_α = 11.03 ± 0.08–11.20 ± 0.05 MeV (full width at half maximum), τ = 0.04–0.52 ms]. The same values for ^{265}Sg and ^{261}Rf in both chains do not contradict the known values for their decay path marked with index "b," e.g., E_α = 8.47 ± 0.05–8.90 ± 0.13 MeV (full width at half maximum) and τ = 2.5–95.3 s for ^{265}Sg^b [26,27,32,33].

The half-life of ^{273}Ds, determined from six decays (Refs. [26,27] and this paper) is $0.18^{+0.11}_{-0.05}$ ms. The decay time of ^{273}Ds in the second (right) chain in Fig. 3 exceeds this value by about two orders of magnitude. The energy of the α particle is also approximately 0.2 MeV lower than the average value of 11.10 MeV (Refs. [26,27] and this paper). In addition, the hindrance factors for these decay branches, derived from experimental and calculated half-lives, are 2.1–2.8 [16,17,20,21] and 1.6 [22] for 11.10-MeV decay and 140–175 [16,17,20,21] and 106 [22] for 10.93-MeV decay. This indicates the observation of a second decay path for ^{273}Ds with $T_{1/2} = 30^{+140}_{-15}$ ms.

Unfortunately, in both chains in Fig. 3, there is no complete information about the decay of ^{269}Hs. However, from the known data for ^{273}Ds and ^{269}Hs, one can plot the energy spectra of their α particles (Fig. 4). The energies of ^{269}Hs measured after the α decay of ^{273}Ds are shown by a full

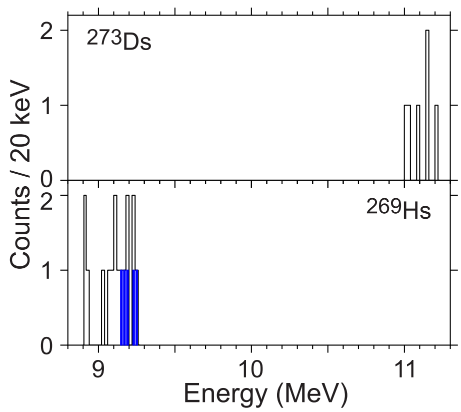

FIG. 4. Alpha-particle energy spectra for ^{273}Ds and ^{269}Hs observed in Refs. [10,26,27] and in this paper (only $E_\alpha = 11.017$ MeV for ^{273}Ds is given). The events observed for ^{269}Hs after α decay of ^{273}Ds in Refs. [26,27] as well as a summary of known data are shown by full (blue) and open histograms, respectively.

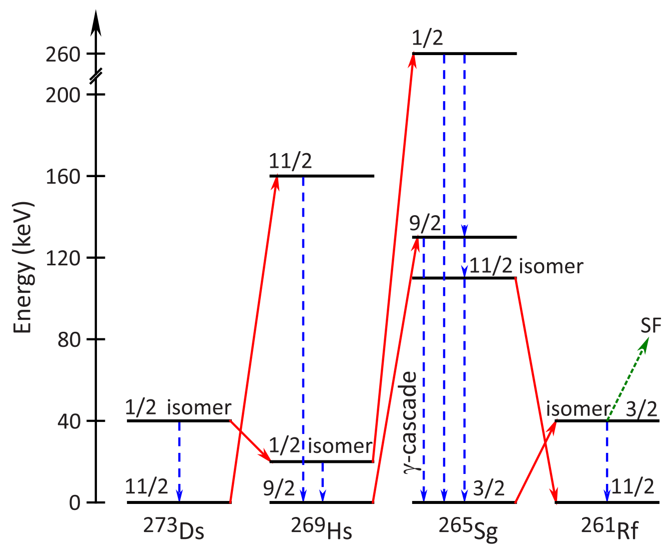

FIG. 5. The one-quasiparticle states and decay patterns for nuclei in the α-decay chain starting from ^{273}Ds.

(blue) histogram. It can be seen that the decay of ^{273}Ds leads mainly to the high-energy part of the spectrum of ^{269}Hs with $E_\alpha = 9.20$ MeV. This suggests the existence of different decay paths for ^{269}Hs as well.

Using the decay pattern proposed in Ref. [32] for ^{269}Hs and descendant nuclei, we have tentatively added its upper part by including new data (see Table III and Fig. 5). We divided the decays of ^{273}Ds and ^{269}Hs into two paths, denoting them with the symbols "a" and "b" as in Refs. [32,33]. The decay from the 10.93-MeV state leads to the SF of $^{261}\mathrm{Rf}^b$, as well as four of the five decays of ^{273}Ds after the decay of ^{277}Cn and the first decay of ^{273}Ds shown in Fig. 3. Since decays of ^{269}Hs may occur through both paths "a" and "b," decays $^{273}\mathrm{Ds}^a \to {}^{269}\mathrm{Hs}^{a,b} \to {}^{265}\mathrm{Sg}^{a,b}$ cannot be unambiguously excluded. In this case, the existence of two states can be assumed for ^{269}Hs: $^{269}\mathrm{Hs}^a$ with $T_{1/2} = 2.8^{+13.6}_{-1.3}$ s (from Fig. 3) and $^{269}\mathrm{Hs}^b$ with $T_{1/2} = 13^{+10}_{-4}$ s (from Refs. [26,27] and this paper).

The modified decay pattern for ^{273}Ds and its decay products is shown in Table III and Fig. 5. It should be noted that for most of the deformed even-Z isotopes with an odd number of neutrons in the ^{273}Ds decay chain, the energy spectra reach several hundred keV (see, e.g., Fig. 4 and Refs. [32,33]), which may indicate a complex scheme of their energy levels and transitions through them. In some cases, the broadening of the peaks may be caused by the insufficiently high energy resolution of the detectors.

As in Refs. [32,33], we show the average energies of α particles for $^{265}\mathrm{Sg}^{a,b}$ and $^{261}\mathrm{Rf}^{a,b}$. For $^{273}\mathrm{Ds}^b$ we give the average α-particle energy determined by the six decays from Refs. [26,27] and this paper. The α-particle energy of $^{269}\mathrm{Hs}^a$ shown in the table was determined from five events that were observed after the α decay of ^{277}Cn [26,27]. The hindrance factor for $^{269}\mathrm{Hs}^a$ is 6.6–7.3 [16,17,20,21] or 9.7 [22]. The average $^{269}\mathrm{Hs}^b$ energy was calculated from three α-decay energies (8.93 and 9.18 MeV [10] and 9.23MeV [26]), after which α decay of $^{261}\mathrm{Rf}^a$ was observed.

The extracted decay pattern for the α-decay chain starting from ^{273}Ds is shown in Fig. 5 (Table III). The present experimental and literature [10,26,27,32,33] data are used for constructing the decay schemes of corresponding isotopes. As seen, the possible ground state 11/2 and low-lying isomeric state 1/2 are populated in ^{273}Ds. The α transition from this isomer populates states with low spins (1/2, 3/2) in ^{269}Hs, ^{265}Sg, ^{261}Rf, and ^{257}No:

$$^{273}\mathrm{Ds}(1/2) \to {}^{269}\mathrm{Hs}(1/2) \to {}^{265}\mathrm{Sg}(3/2) \to {}^{261}\mathrm{Rf}(3/2) \to \mathrm{SF}, \alpha.$$

TABLE III. The same as Table II but for ^{273}Ds.

Nucleus	Decay mode	$T_{1/2}^{\mathrm{exp}}$	E_α (MeV)	Q_α (MeV)	Spin	T_a^{calc}	$T_{\mathrm{SF}}^{\mathrm{calc}}$
$^{273}\mathrm{Ds}^a$	α	30^{+140}_{-15} ms	10.93(2)	11.09(2)	11/2	87 ms	110 s
$^{273}\mathrm{Ds}^b$	α	$0.18^{+0.11}_{-0.05}$ ms	11.10(7)	11.27(7)	1/2	0.21 ms	47 s
$^{269}\mathrm{Hs}^a$	α	13^{+10}_{-4} s	9.20(4)	9.34(4)	9/2	15 s	2.2 h
$^{269}\mathrm{Hs}^b$	α	$2.8^{+13.6}_{-1.3}$ s	9.08(15)	9.22(15)	1/2	3 s	14 min
$^{265}\mathrm{Sg}^a$	α	$8.5^{+2.6}_{-1.6}$ s	8.84(5)	8.97(5)	11/2	11 s	14 h
$^{265}\mathrm{Sg}^b$	α	$14.4^{+3.7}_{-2.5}$ s	8.69(5)	8.82(5)	3/2	12 s	59 min
$^{261}\mathrm{Rf}^a$	α	68 ± 3 s	8.28(2)	8.41(2)	11/2	87 s	12 min
$^{261}\mathrm{Rf}^b$	SF	$2.6^{+0.7}_{-0.5}$ s	8.51(6)	8.64(6)	3/2	7.4 s	3.7 s

Because the low-spin state has a smaller hindrance to the SF and the last one competes with α decay, the fission occurs from isomeric state 3/2 in ^{261}Rf. The α decay from the ground state 11/2 in ^{273}Ds leads to the population of states with relatively high spins (9/2, 11/2) in ^{269}Hs and low spins (1/2, 3/2) in ^{265}Sg and ^{261}Rf:

$$^{273}\mathrm{Ds}(11/2) \to {}^{269}\mathrm{Hs}(9/2) \to {}^{265}\mathrm{Sg}(3/2) \to {}^{261}\mathrm{Rf}(3/2) \to \mathrm{SF}, \alpha.$$

In this chain, the transition from the high-spin state 9/2 to the low-spin state 3/2 occurs in ^{265}Sg, where the ground state 3/2 is abundantly populated through the cascade of γ quanta from the excited state 9/2. Since there is also a weak γ-decay branch 9/2 → 11/2 in ^{265}Sg, the α transitions

$$^{273}\mathrm{Ds}(11/2) \to {}^{269}\mathrm{Hs}(9/2) \to {}^{265}\mathrm{Sg}(11/2) \to {}^{261}\mathrm{Rf}(11/2) \to \alpha$$

through the high-spin states only lead to α decay from the ground state 11/2 of ^{261}Rf. Thus, these decay chains mentioned above are finished by the SF or α decay of ^{261}Rf(3/2) and α decay of ^{261}Rf(11/2). Such an SF branch from the low-spin isomeric state is measured in the present experiments and Refs. [10,26,27,32,33]. As seen in Fig. 5, there are four isomeric states: ^{273}Ds(1/2), ^{269}Hs(1/2), ^{265}Sg(11/2), and ^{261}Rf(3/2). So, the states $^{265}\mathrm{S\,g}^{a}$ ($^{261}\mathrm{R\,f}^{a}$) and $^{265}\mathrm{S\,g}^{b}$ ($^{261}\mathrm{R\,f}^{b}$) in Refs. [32,33] are the isomeric (ground) 11/2 and ground (isomeric) 3/2 states, respectively, in Fig. 5. It should be emphasized that the isomeric states ^{273}Ds(1/2), ^{265}Sg(11/2), and ^{261}Rf(3/2) and their decay patterns are predicted in Ref. [34]. The predictions of isomeric states ^{273}Ds(1/2) and ^{269}Hs(1/2) are also given in Ref. [25]. For the ^{261}Rf, the ground and isomeric states in Ref. [35] are also the one-quasiparticle states with spins 11/2 and 3/2, respectively. Since the energies of the ground and isomeric states are close to each other, the direct production of ^{265}Sg or ^{261}Rf as evaporation residues populates both states with similar intensity, as observed in the experiment [33].

The production cross sections of nuclei in the ^{232}Th + ^{48}Ca and ^{238}U + ^{40}Ar reactions measured in this paper are shown in Fig. 6. This figure also shows the results of the first ^{232}Th + ^{48}Ca experiment at three low excitation energies of the ^{280}Ds compound nucleus [1]. As can be seen, the cross sections of the 5n reaction channels at $E^* \approx 50$ MeV are similar within the experimental uncertainties.

The ^{232}Th(^{48}Ca, $3-5n$)$^{275\text{–}277}$Ds reaction cross sections are in agreement with the calculations published in Ref. [37]. But it turned out to be difficult for us to find the results of calculations of the cross sections for reactions of actinide nuclei with ^{40}Ar in the literature. In one case [38], the calculated cross sections for reactions with ^{48}Ca are in good agreement with experimental data. But the cross section for the ^{247}Bk + ^{40}Ar reaction at excitation energies below the fusion barrier ($B_{\mathrm{Bass}} = 39.4$ MeV) seems to be too optimistic, e.g., about 100 pb for the 2n channel at $E^* = 30$ MeV.

The cross-section values measured in this paper are consistent with the conclusion made in Ref. [39] based on a comparison of calculated cross sections for the ^{251}Cf + ^{40}Ar and ^{243}Cm + ^{48}Ca reactions leading to the same compound

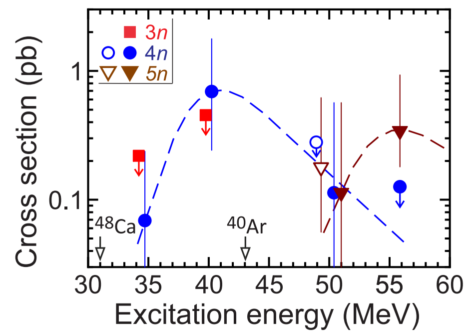

FIG. 6. Cross sections for the 3n- to 5n-evaporation channels for the ^{232}Th + ^{48}Ca (closed symbols, Ref. [1] and this paper) and ^{238}U + ^{40}Ar (open symbols, this paper) reactions. Vertical error bars correspond to total uncertainties. The symbols with arrows show the upper cross-section limits. The dashed lines through the data are drawn to guide the eye. The Bass barriers [36] are shown by open arrows for comparison.

nucleus: "…the use of an ^{40}Ar beam is less favorable as compared with ^{48}Ca. This is owing to much 'hotter' character of the ^{40}Ar + ^{251}Cf fusion reaction (only the cross sections for the 5n evaporation channels are comparable for both reactions)."

In this series of experiments on the synthesis of Ds isotopes in the transition region, we have filled in the missing link and obtained an impressive picture of the dependence of the stability of the superheavy nucleus relative to α decay on the number of neutrons. In Fig. 7, we show the partial α-decay half-lives of nine Ds isotopes synthesized in these experiments, as well as in the cold-fusion ^{208}Pb + ^{62,64}Ni and ^{70}Zn and the hot-fusion ^{240,242,244}Pu + ^{48}Ca reactions (see Refs. [1,4,6,16,19,26,27,40,41] and references therein). For comparison, we show the results of calculations obtained 30 years ago, ten years before the appearance of the first

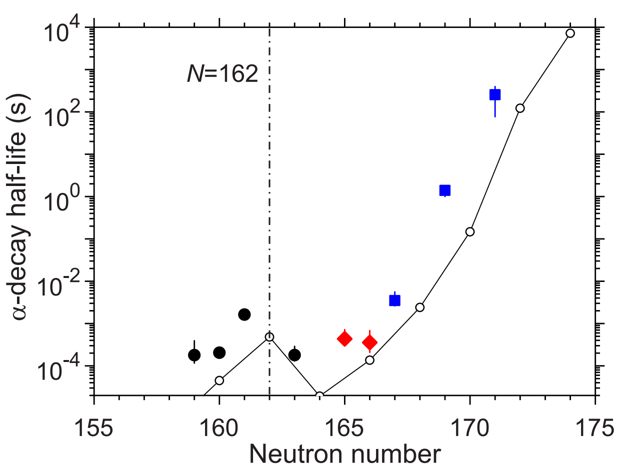

FIG. 7. Partial half-lives T_α vs neutron number for the isotopes of Ds. The results from the cold-fusion and ^{48}Ca-induced reactions are shown by black circles and blue squares, respectively; the results for ^{276}Ds [1] and ^{275}Ds from this paper are shown by red diamonds. The results of calculations [42] are shown by open circles connected by lines.

experimental data on the synthesis of superheavy elements in reactions with ^{48}Ca [42]. It can be seen that the stability of the Ds isotopes varies greatly. The small growth in the region of $N = 162$ is due to the action of the deformed shell. In the region with $N > 162$, the decrease in the half-life is associated with a weakening of the stabilizing effect of the shell $N = 162$ as it moves away from it into the region of a larger number of neutrons. Then, in the region with $N \geqslant 165$, the stability of the Ds isotopes increases, faster than for other elements (see, e.g., Fig. 11 in Ref. [41] and Fig. 4 in Ref. [1]), which clearly indicates a much stronger effect of the next neutron shell. In theory, this is explained by the action of a closed spherical shell $N = 184$. Despite the fact that the heaviest isotope, ^{281}Ds ($N = 171$), obtained experimentally as a grand product of the α decay of ^{289}Fl, is 13 neutrons away from $N = 184$, its stability exceeds the stability of the Ds isotopes with $N \approx 162$ by five orders of magnitude. As follows from the theoretical predictions (see Fig. 7), with an increase in the number of neutrons in the Ds nucleus, a further increase in stability is expected.

The heavy isotope ^{282}Ds is the product of the $2n$-reaction channel of ^{48}Ca with ^{244}Pu and ^{248}Cm and the subsequent α decay of ^{290}Fl and ^{294}Lv, respectively. However, the cross section of these reactions seems to be lower than that of the $3n$ channel, since in a number of experiments the products of the $2n$ channel were not observed. In addition, spontaneous fission of ^{286}Cn may be more likely than its α decay. For the synthesis of Ds isotopes with $N>172$, there are no interacting nuclei with a neutron excess larger than in ^{244}Pu, ^{248}Cm, and ^{48}Ca. It is even more difficult to synthesize such nuclei in transfer reactions such as $^{238}\mathrm{U} + {}^{238}\mathrm{U}$ or $^{238}\mathrm{U} + {}^{248}\mathrm{Cm}$ (see, e.g., Ref. [43]). Therefore, returning to the fusion reaction $^{248}\mathrm{Cm} + {}^{48}\mathrm{Ca}$, previously used for the synthesis of Lv isotopes, one can consider rare deexcitation channels of the compound nucleus ^{296}Lv by evaporation of a minimum number of neutrons or by the emission of charged particles (p or α).

To date, more than 500 decay chains of superheavy nuclei have been synthesized in various laboratories around the world. The products of the *pxn* channel were definitely not observed in these experiments. However, theoretical calculations predict the cross section of the *pxn* channel for, e.g., the $^{248}\mathrm{Cm} + {}^{48}\mathrm{Ca}$ reaction at a level that is attainable at the present time, for example, $\sigma_{p2n} \approx 60$ fb [44], $\sigma_{p(2-3)n} \approx 200$ fb [45], $\sigma_{p3n} \approx 30$ fb [46], and $\sigma_{p1n} \approx 60$ fb [47].

The decay properties of ^{293}Mc are of great interest. It contains three more neutrons than the heaviest known isotope, ^{290}Mc, a daughter nucleus of ^{294}Ts synthesized in the $^{249}\mathrm{Bk} + {}^{48}\mathrm{Ca}$ reaction. The isotope ^{293}Mc can predominantly undergo α decay with an energy $Q_\alpha \approx 10.1$ MeV and a half-life of several seconds. Its daughter product will be an unknown heavy isotope, ^{289}Nh ($N = 176$), which is also likely to be an α emitter with $Q_\alpha \approx 9.4$ MeV and a half-life of several minutes. The second α decay leads to ^{285}Rg ($N = 174$) with a half-life of about 1 h. The electron capture of $^{285}\mathrm{Rg(EC)} \rightarrow {}^{285}$Ds ($N = 175$) can compete with the emission of the α particle. The resulting even-Z ^{285}Ds can undergo both α decay and spontaneous fission, with a half-life of one month. It is obvious that the observation of such nuclei is a serious challenge. Unfortunately, it is impossible to synthesize such nuclei by all other known methods of artificial synthesis of chemical elements. But this is the way to centenarians at the top of the island of stability. Their decay properties provide valuable information about the strength of the stabilizing effect of the closed neutron shell $N = 184$ in its immediate vicinity.

IV. SUMMARY

The $^{232}\mathrm{Th} + {}^{48}\mathrm{Ca}$ reaction has been studied at the separator DGFRS-2. The new nuclide ^{275}Ds, a product of the $5n$ channel, with a half-life of $0.43^{+0.29}_{-0.12}$ ms and α-particle energy of 11.20 MeV, was synthesized for the first time. The decays of this nucleus led to the previously synthesized daughter nuclei ^{271}Hs, ^{267}Sg, and ^{263}Rf, which means the first observation and identification of the superheavy nucleus, the product of the fusion of ^{48}Ca with the actinide nuclide, by the method of genetic correlations with known nuclei.

The decay properties of the daughter nuclei ^{271}Hs, ^{267}Sg, and ^{263}Rf, measured in previous studies [10] and in this paper, indicate the presence of transitions through different energy levels. One of the branches of ^{271}Hs with low α-particle energy ($E_\alpha = 9.05$ MeV) leads to SF of ^{267}Sg, and the second, with higher energy ($E_\alpha = 9.34$ MeV), leads to α decay of ^{267}Sg, followed by fission of ^{263}Rf. The cross sections of the $^{232}\mathrm{Th}(^{48}\mathrm{Ca}, 5n)^{275}\mathrm{Ds}$ reaction of $0.11^{+0.46}_{-0.09}$ and $0.34^{+0.59}_{-0.16}$ pb were measured at excitation energies $E^* = 51$ and 56 MeV due to observation of one and five decay chains, respectively.

In the $^{238}\mathrm{U}(^{40}\mathrm{Ar}, 5n)$ reaction, two decay chains of ^{273}Ds were observed. The decay properties of the nuclei in one of them are in good agreement with the properties of the nuclei measured in the five decay chains of the parent nucleus ^{277}Cn [26,27] produced in the cold-fusion reaction $^{208}\mathrm{Pb}(^{70}\mathrm{Zn}, 1n)$. In the second chain, the energy of the α particle of ^{273}Ds turned out to be approximately 200 keV lower than that measured for ^{273}Ds ($E_\alpha \approx 11.10$ MeV), and the decay time (41.7 ms) is two orders of magnitude higher than its average decay time ($T_{1/2} = 0.18^{+0.11}_{-0.05}$ ms), determined from six decays. Based on these results, the working hypothesis of the isotope decay pattern proposed in Ref. [32] has been supplemented with the isotopes ^{273}Ds and ^{269}Hs. The cross section of the $5n$-evaporation channel of the $^{238}\mathrm{U} + {}^{40}\mathrm{Ar}$ reaction at $E^* = 49$ MeV of $0.18^{+0.44}_{-0.12}$ pb was found to be comparable to that for the production of ^{275}Ds at close excitation energy.

The decay schemes for the isotopes stemming from α decay of ^{273,275}Ds were extracted by using the experimental Q_α and $T_{\alpha,\mathrm{SF}}$ values and fission model [23,24]. The SF from low-spin isomeric $^{261}\mathrm{Rf}(3/2)$ and ground $^{263}\mathrm{Rf}(1/2)$ states, and the existence of low-lying isomeric states in the nuclei ^{261,263}Rf, ^{265,267}Sg, ^{269,271}Hs, and ^{273}Ds, were proposed.

ACKNOWLEDGMENTS

We thank the personnel operating the DC280 cyclotron and the associates of the ion-source group for obtaining ^{48}Ca and ^{40}Ar beams. These studies were supported by the Ministry of Science and Higher Education of the Russian Federation through Grant No. 075-10-2020-117 and by a JINR Directorate grant. This work was also supported by the Strategic Priority Research Program of Chinese Academy of Sciences (Grant No. XDB34010000).

[1] Yu. Ts. Oganessian, V. K. Utyonkov, M. V. Shumeiko, F. Sh. Abdullin, S. N. Dmitriev, D. Ibadullayev *et al.*, New isotope ^{276}Ds and its decay products ^{272}Hs and ^{268}Sg from the ^{232}Th + ^{48}Ca reaction, Phys. Rev. C **108**, 024611 (2023).

[2] Yu. Ts. Oganessian *et al.*, DGFRS-2: A gas-filled recoil separator for the Dubna Super Heavy Element Factory, Nucl. Instrum. Methods Phys. Res. A **1033**, 166640 (2022).

[3] G. G. Gulbekian *et al.*, Start-up of the DC-280 cyclotron, the basic facility of the factory of superheavy elements of the laboratory of nuclear reactions at the joint institute for nuclear research, Phys. Part. Nucl. Lett. **16**, 866 (2019).

[4] F. G. Kondev, M. Wang, W. J. Huang, S. Naimi, and G. Audi, The NUBASE2020 evaluation of nuclear physics properties, Chin. Phys. C **45**, 030001 (2021).

[5] W. D. Myers and W. J. Swiatecki, Nuclear properties according to the Thomas-Fermi model, Nucl. Phys. A. **601**, 141 (1996).

[6] Yu. Ts. Oganessian, V. K. Utyonkov, D. Ibadullayev, F. Sh. Abdullin, S. N. Dmitriev, M. G. Itkis *et al.*, Investigation of ^{48}Ca-induced reactions with ^{242}Pu and ^{238}U targets at the JINR superheavy element factory, Phys. Rev. C **106**, 024612 (2022).

[7] Yu. Ts. Oganessian, V. K. Utyonkov, N. D. Kovrizhnykh, F. Sh. Abdullin, S. N. Dmitriev, A. A. Dzhioev *et al.*, New isotope ^{286}Mc produced in the ^{243}Am + ^{48}Ca reaction, Phys. Rev. C **106**, 064306 (2022).

[8] Yu. Ts. Oganessian, V. K. Utyonkov, N. D. Kovrizhnykh, F. Sh. Abdullin, S. N. Dmitriev, D. Ibadullayev *et al.*, First experiment at the super heavy element factory: High cross section of ^{288}Mc in the ^{243}Am + ^{48}Ca reaction and identification of the new isotope ^{264}Lr, Phys. Rev. C **106**, L031301 (2022).

[9] D. Ibadullayev, Yu. S. Tsyganov, A. N. Polyakov, A. A. Voinov, and M. V. Shumeiko, Flexible scenario for background suppression in heavy element research, Phys. At. Nucl **85**, 1981 (2022).

[10] J. Dvorak, W. Brüchle, M. Chelnokov, R. Dressler, Ch. E. Düllmann, K. Eberhardt *et al.*, Doubly magic nucleus $^{270}_{108}$Hs$_{162}$, Phys. Rev. Lett. **97**, 242501 (2006); J. Dvorak, W. Brüchle, M. Chelnokov, Ch. E. Düllmann, Z. Dvorakova, K. Eberhardt *et al.*, Observation of the 3n evaporation channel in the complete hot-fusion reaction ^{26}Mg + ^{248}Cm leading to the new superheavy nuclide ^{271}Hs, **100**, 132503 (2008).

[11] S. Hofmann, S. N. Dmitriev, C. Fahlander, J. M. Gates, J. B. Roberto, and H. Sakai, On the discovery of new elements, Pure Appl. Chem. **90**, 1773 (2018).

[12] J. V. Kratz *et al.*, An EC-branch in the decay of 27-s ^{263}Db: Evidence for the isotope ^{263}Rf, Radiochim. Acta **91**, 59 (2003).

[13] K.-H. Schmidt, C.-C. Sahm, K. Pielenz, and H.-G. Clerc, Some remarks on the error analysis in the case of poor statistics, Z. Phys. A **316**, 19 (1984).

[14] V. B. Zlokazov, Program for constructing the estimates of the parameter of the exponential distribution under conditions of poor statistics, Nucl. Instrum. Methods **151**, 303 (1978).

[15] K. H. Schmidt, A new test for random events of an exponential distribution, Eur. Phys. J. A **8**, 141 (2000).

[16] Yu. Ts. Oganessian, V. K. Utyonkov, Yu. V. Lobanov, F. Sh. Abdullin, A. N. Polyakov, I. V. Shirokovsky *et al.*, Measurements of cross sections and decay properties of the isotopes of elements 112, 114, and 116 produced in the fusion reactions ^{233,238}U, ^{242}Pu, and ^{248}Cm + ^{48}Ca, Phys. Rev. C **70**, 064609 (2004).

[17] C. Qi, F. R. Xu, R. J. Liotta, R. Wyss, M. Y. Zhang, C. Asawatangtrakuldee, and D. Hu, Microscopic mechanism of charged-particle radioactivity and generalization of the Geiger-Nuttall law, Phys. Rev. C **80**, 044326 (2009).

[18] D. Rudolph *et al.*, Spectroscopy of element 115 decay chains, Phys. Rev. Lett. **111**, 112502 (2013).

[19] A. Såmark-Roth *et al.*, Spectroscopy along flerovium decay chains. III. Details on experiment, analysis, ^{282}Cn, and spontaneous fission branches, Phys. Rev. C **107**, 024301 (2023).

[20] Yang-Yang Xu, De-Xing Zhu, Xun Chen, Biao He Xi-JunWu, and Xiao-Hua Li, A unified formula for α decay half-lives, Eur. Phys. J. A **58**, 163 (2022).

[21] M. Ismail, A. Y. Ellithi, A. Adel, and M. A. Abbas, An improved unified formula for α-decay and cluster radioactivity of heavy and superheavy nuclei, Eur. Phys. J. A **58**, 225 (2022).

[22] Song Luo, Yang-Yang Xu, De-Xing Zhu, Biao He, Peng-Cheng Chu, and Xiao-Hua Li, Improved Geiger-Nuttall law for α-decay half-lives of heavy and superheavy nuclei, Eur. Phys. J. A **58**, 244 (2022).

[23] I. S. Rogov, G. G. Adamian, and N. V. Antonenko, Dynamics of a dinuclear system in charge-asymmetry coordinates: A decay, cluster radioactivity, and spontaneous fission, Phys. Rev. C **100**, 024606 (2019); Cluster approach to spontaneous fission of even-even isotopes of U, Pu, Cm, Cf, Fm, No, Rf, Sg, and Hs, **104**, 034618 (2021).

[24] I. S. Rogov, G. G. Adamian, and N. V. Antonenko, Spontaneous fission hindrance in even-odd nuclei within a cluster approach, Phys. Rev. C **105**, 034619 (2022).

[25] G. G. Adamian, N. V. Antonenko, A. N. Bezbakh, and R. V. Jolos, Effect of properties of superheavy nuclei on their production and decay, Phys. Part. Nucl. **47**, 387 (2016); G. G. Adamian, N. V. Antonenko, L. A. Malov, and H. Lenske, Examination of production and properties of $^{268–271}$Hs, Phys. Rev. C **96**, 044310 (2017).

[26] S. Hofmann *et al.*, New results on elements 111 and 112, Eur. Phys. J. A **14**, 147 (2002).

[27] T. Sumita *et al.*, New result on the production of ^{277}Cn by the ^{208}Pb + ^{70}Zn reaction, J. Phys. Soc. Jpn. **82**, 024202 (2013).

[28] Yu. Ts. Oganessian, V. K. Utyonkov, F. Sh. Abdullin, S. N. Dmitriev, R. Graeger, R. A. Henderson *et al.*, Synthesis and study of decay properties of the doubly magic nucleus ^{270}Hs in the ^{226}Ra + ^{48}Ca reaction, Phys. Rev. C **87**, 034605 (2013).

[29] R. Graeger, D. Ackermann, M. Chelnokov, V. Chepigin, Ch. E. Düllmann, J. Dvorak *et al.*, Experimental study of the ^{238}U(^{36}S, $3-5n$)$^{269–271}$Hs reaction leading to the observation of ^{270}Hs, Phys. Rev. C **81**, 061601(R) (2010).

[30] K. Nishio *et al.*, Nuclear orientation in the reaction ^{34}S + ^{238}U and synthesis of the new isotope ^{268}Hs, Phys. Rev. C **82**, 024611 (2010).

[31] F. P. Heβberger, Spontaneous fission properties of superheavy elements, Eur. Phys. J. A **53**, 75 (2017).

[32] Ch. E. Düllmann and A. Türler, ^{248}Cm(^{22}Ne, xn)$^{270-x}$Sg reaction and the decay properties of ^{265}Sg reexamined, Phys. Rev. C **77**, 064320 (2008).

[33] H. Haba, D. Kaji, Y. Kudou, K. Morimoto, K. Morita, K. Ozeki *et al.*, Production of ^{265}Sg in the ^{248}Cm(^{22}Ne, 5n)^{265}Sg reaction and decay properties of two isomeric states in ^{265}Sg, Phys. Rev. C **85**, 024611 (2012).

[34] L. A. Malov, A. N. Bezbach, G. G. Adamian, N. V. Antonenko, and R. V. Jolos, Electromagnetic transitions between low-lying nonrotational states of odd-neutron nuclei in α-decay chains starting from ^{265,267,269}Hs, Phys. Rev. C **106**, 034302 (2022).

[35] A. Parkhomenko and A. Sobiczewski, Neutron one-quasiparticle states of heaviest nuclei, Acta Phys. Pol. B **36**, 3115 (2005).
[36] R. Bass, Fusion reactions: Successes and limitations of a one-dimensional description, in *Proceedings of the Symposium on Deep Inelastic and Fusion Reactions with Heavy Ions, West Berlin, 1979*, edited by W. von Oertzen, Lecture Notes in Physics Vol. 117 (Springer-Verlag, Berlin, 1980), p. 281.
[37] J. Hong, G. G. Adamian, N. V. Antonenko, M. Kowal, and P. Jachimowicz, Isthmus connecting mainland and island of stability of superheavy nuclei, Phys. Rev. C **106**, 014614 (2022).
[38] P.-H. Chen, H. Wu, Z.-X. Yang, X.-H. Zeng, and Z.-Q. Feng, Prediction of synthesis cross sections of new moscovium isotopes in fusion-evaporation reactions, Nucl. Sci. Tech. **34**, 7 (2023).
[39] V. I. Zagrebaev and W. Greiner, Cross sections for the production of superheavy nuclei, Nucl. Phys. A. **944**, 257 (2015).
[40] S. Hofmann, Superheavy elements, Lect. Notes Phys. **764**, 203 (2009).
[41] Yu. Ts. Oganessian and V. K. Utyonkov, Superheavy nuclei from ^{48}Ca-induced reactions, Nucl. Phys. A. **944**, 62 (2015).
[42] R. Smolańczuk, J. Skalski, and A. Sobiczewski, Spontaneous-fission half-lives of deformed superheavy nuclei, Phys. Rev. C **52**, 1871 (1995).
[43] V. V. Saiko and A. V. Karpov, Analysis of multinucleon transfer reactions with spherical and statically deformed nuclei using a Langevin-type approach, Phys. Rev C **99**, 014613 (2019).
[44] J. Hong, G. G. Adamian, and N. V. Antonenko, Ways to produce new superheavy isotopes with $Z = 111$–117 in charged particle evaporation channels, Phys. Lett. B **764**, 42 (2017).
[45] K. Siwek-Wilczyńska, T. Cap, and M. Kowal, Exploring the production of new superheavy nuclei with proton and α-particle evaporation channel, Phys. Rev. C **99**, 054603 (2019).
[46] J. Hong, G. G. Adamian, N. V. Antonenko, P. Jachimowicz, and M. Kowal, Possibilities of direct production of superheavy nuclei with $Z = 112-118$ in different evaporation channels, Phys. Lett. B **809**, 135760 (2020).
[47] N. Yu. Kurkova and A. V. Karpov, Perspectives of synthesis of some new superheavy nuclei, Phys. At. Nucl. **86**, 311 (2023).